Stochastic Dissipative Euler's equations for a free body

J.A. de la Torre, J. Sánchez-Rodríguez, Pep Español[1]

[1] *Dept. Física Fundamental, Universidad Nacional de Educación a Distancia, Madrid, Spain*

(Dated: August 21, 2024)

Intrinsic thermal fluctuations within a real solid challenge the rigid body assumption that is central to Euler's equations for the motion of a free body. Recently, we have introduced a dissipative and stochastic version of Euler's equations in a thermodynamically consistent way (European Journal of Mechanics - A/Solids 103, 105184 (2024)). This framework describes the evolution of both orientation and shape of a free body, incorporating *internal* thermal fluctuations and their concomitant dissipative mechanisms. In the present work, we demonstrate that, in the absence of angular momentum, the theory predicts that the principal axes unit vectors of a body undergo an anisotropic Brownian motion on the unit sphere, with the anisotropy arising from the body's varying moments of inertia. The resulting equilibrium time correlation function of the principal eigenvectors decays exponentially. This theoretical prediction is confirmed in molecular dynamics simulations of small bodies. The comparison of theory and *equilibrium* MD simulations allow us to measure the orientational diffusion tensor. We then use this information in the Stochastic Dissipative Euler's Equations, to describe a *non-equilibrium* situation of a body spinning around the unstable intermediate axis. The agreement between theory and simulations is excellent, offering a validation of the theoretical framework.

I. INTRODUCTION

The motion of a rigid body in free space is governed by Euler's equations which assume that the distance between the constituent particles is constant [1, 2]. This idealization overlooks the inherent elasticity of solids as well as the thermal motion that all particles within a body experience at finite temperatures. While Euler's equations have been used for centuries to describe rotational dynamics, they fall short in explaining certain dissipative phenomena observed in nature like precession relaxation or tidal locking. Under precession relaxation, free spinning bodies always end up rotating around the major axis of inertia, explaining why 98% of asteroids are spinning in pure rotation [3–5]. Tidal locking describes how a gravitationally bonded body ends up synchronizing its orbital and rotational periods, as in the case of our Moon. From a conceptual point of view, Euler's equations can be obtained under the rigid body idealization from the relationship between two orthogonal reference systems in motion, the observation that the inertia tensor diagonalizes in the principal axes reference system, and the conservation laws, in particular that of angular momentum [6, 7]. However, until recently, the link between the Hamiltonian motion of the particles constituting the body and Euler's equations for the motion of the body was lacking. This missing link has been addressed in Ref. [8]. To "derive" Euler's equations from Hamilton's equations one needs to resort to the powerful machinery of the Theory of Coarse-Graining, also known as Non-Equilibrium Statistical Mechanics and, some times, as the Mori-Zwanzig projector operator method [10–14]. In this theory, following Gibbs [15] one introduces the notions of microstates and macrostates. The macrostates, or coarse-grained (CG) variables, define the coarse-grained level of description of the system. The theory makes the fundamental modelling assumption that the selected CG variables evolve in two distinct time scales, one characterized by small and fast contribution due to collisions/vibrations which is modelled as white noise, and another slow contribution due to the cumulative effect of these rapid contributions. In this way, the theory describes the evolution of the CG variables as a diffusive Markov process [10, 11]. One possible level of description for the motion of a quasi-rigid body would consider the body as a continuum, and use the displacement and velocity fields as CG variables, to produce a viscoelastic field description (including free boundary conditions) of the free body. In the present work, however, we consider a coarser level of description, closer to the original Euler's description, which takes the gyration tensor as the primary variable. The gyration tensor is closely related to the inertia tensor and its eigenvectors (defining the principal axes) describe the orientation of the body, while the eigenvalues (referred to as central moments) describe the overall shape of the body.

In Ref. [8], we have constructed from first principles the stochastic differential equations that govern the evolution of the orientation and shape of a quasi-rigid body. These equations, referred to as Stochastic Dissipative Euler's Equations (SDEE), generalize Euler's equations in order to include thermal fluctuations and its associated dissipation. The reversible part of these equations is given by the usual Euler's equations, while the newly derived dissipative part of the dynamics contains two dissipative mechanisms: an orientational diffusion of the principal axes, and a dilational friction damping the oscillations in the central moments. In addition, the SDEE describe the random motion of the eigenvectors and eigenvalues due to thermal fluctuations.

For macroscopic bodies, thermal fluctuations become negligible. However, dissipation cannot be neglected in general. In Ref. [16], we have studied numerically the ordinary differential equations that result from neglecting

thermal fluctuations in the SDEE. By switching on and off the different dissipative mechanisms involved, we gave support to the claim that precession relaxation is due to orientational diffusion rather than dilational friction. In fact, Euler's equations predict that the motion of a body spinning around the intermediate axis of inertia is unstable [17–19], a result known as the tennis racket theorem or the intermediate axis theorem. As a consequence, a free body experiences the Dzhanibekov effect, a striking phenomena in which the intermediate axis performs 180^0 degrees flips in a periodic way. When dissipation is included in the description, the Dzhanibekov effect dissapears as a consequence of precession relaxation. In the process, "organized" rotational kinetic energy is transformed into "disorganized" internal thermal energy while increasing the entropy of the system, and consequently heating the body. The resulting minimum kinetic energy occurs when the body is spinning around the axis of larger moment of inertia.

In the present paper, we turn our attention to the Stochastic Dissipative Euler's equations including thermal fluctuations as formulated in [8]. The objective of the paper is to compare the predictions of this theory with Molecular Dynamics simulations of a free body composed of bonded interacting atoms, see Fig. 1. This constitutes a stringent test of the theory and constitutes a necessary validation step. The SDEE encompasses several parameters that must be determined to enable numerical solutions and generate predictions. The list of these parameters include the average central moments giving the size and geometry of the body, an elastic matrix defined in terms of the covariance of the central moments, and two sets of dissipative coefficients: an orientational diffusion matrix and a dilational friction matrix. The values of these parameters are obtained from *equilibrium* MD simulations of the body at zero angular momentum. The test phase of the procedure is to predict *non-equilibrium* results about precession relaxation using these previously determined set of parameters.

In this paper, we further elucidate a theoretical insight concerning the SDEE derived in [8]. We demonstrate that when the angular momentum of the body vanishes, the principal axes follow an anisotropic Brownian motion on the unit sphere. In this way, a body of nanoscopic dimensions with zero angular momentum will explore all possible orientations [20]. Loosely speaking the body "spins" without angular momentum. The key observation is that the movement of the principal axes aligns with the mathematically precise concept of spherical Brownian motion [21, 22]. The anisotropic behavior is due to the distinct moments of inertia, which introduce a directional bias in the Brownian motion. This bias reflects the principle that larger moments of inertia result in slower rotational motion around the corresponding axis. We stress that the physical origin of the rotational Brownian motion of a free body is the intrinsic thermal fluctuations of the particles that constitute it. This is physically different from the usual Brownian Rotor, where a particle

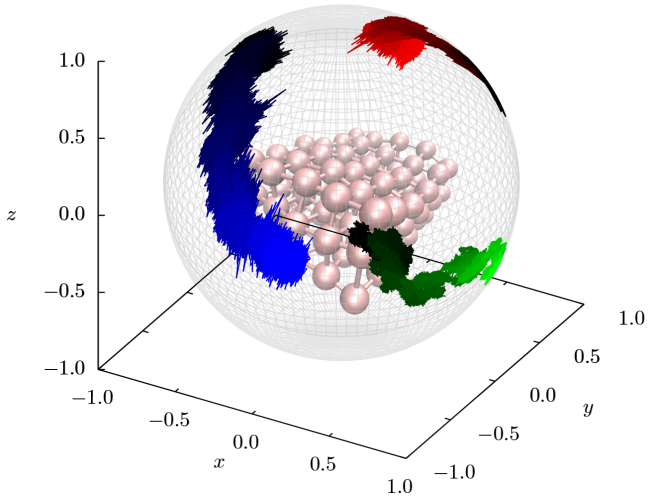

FIG. 1: A small crystal of size $6 \times 5 \times 3$ atoms is simulated with MD. The traces of the three unit principal vectors (in red, green, blue) have darker colors corresponding to earlier times. We demonstrate that these traces can be modelled as realizations of anisotropic Brownian motion on the unit sphere surface.

immersed in a fluid experiences Brownian motion due to the bombardment of the surrounding molecules [23–27].

As the motion of the principal axes is a spherical Brownian motion, we predict that the time-correlation function of the principal vectors decays in a matrix exponential form. We compare this prediction with the MD simulation results, finding excellent agreement. The exponential matrix contains the orientational diffusion coefficients, and the fitting against the equilibrium MD simulation results allow us to determine these parameters.

The paper is organized as follows. In Sec. II we summarize the main result of Ref. [8] which is the SDEE. In Sec III we consider the SDEE when the angular momentum of the system is zero, and show that the motion of the principal axes correspond to an anisotropic Brownian motion. The details of the mathematical description of anisotropic Brownian motion are given in Appendix VII. In Sec. IV we run equilibrium MD simulations of a small body, and measure all the required parameters in the SDEE. In Sec. V, we compare the numerical predictions of the SDEE with the results of non-equilibrium MD simulations in which the body is set into motion through an "angular kick" that suddenly sets a body initially at rest into a rotation along the intermediate axis. We compare the evolution of the rotation kinetic energy, reflecting precession relaxation, in the mesoscopic and microscopic simulations, obtaining excellent agreement. Finally, in Sec. VI we present our conclusions.

II. THE MOTION OF A QUASI-RIGID FREE BODY

In this section, we summarize the theory presented in Ref. [8] for the motion of a quasi-rigid free body. This allow us to set up the notation used in the paper. The body, which is composed of particles bonded with a potential, is described at a coarse-grained level with the center of mass position $\hat{\mathbf{R}}$ and gyration tensor $\hat{\mathbf{G}}$, closely related to the inertia tensor $\hat{\mathbf{I}}$. These CG variables capture how the particles of the body distribute in space, the first giving the "location" of the body and the latter giving a sense of its "shape and orientation". These variables are the ones used to describe a rigid body in Classical Mechanics under the rigid constraint assumption, and it is natural to use these phase functions as CG variables. The gyration tensor is defined as

$$\hat{\mathbf{G}} \equiv \frac{1}{4}\sum_i m_i \left(\mathbf{r}_i - \hat{\mathbf{R}}\right)\left(\mathbf{r}_i - \hat{\mathbf{R}}\right)^T \tag{1}$$

where the superscript T denotes the transpose matrix. The prefactor $1/4$ in the definition (1) allowed us in [8] to interpret directly the eigenvalues $\hat{M}_\alpha$ of $\hat{\mathbf{G}}$ as "dilational masses", or inertia to dilations. The inertia tensor $\hat{\mathbf{I}}$ is defined as

$$\hat{\mathbf{I}} \equiv \sum_i^N m_i [\mathbf{r}_i - \hat{\mathbf{R}}]_\times^T \cdot [\mathbf{r}_i - \hat{\mathbf{R}}]_\times \tag{2}$$

where $[\mathbf{u}]_\times$ is the cross-product matrix formed from a vector $\mathbf{u}$. The action of the cross product matrix on an arbitrary vector $\mathbf{v}$ gives the cross product of both vectors $[\mathbf{u}]_\times \cdot \mathbf{v} = \mathbf{u} \times \mathbf{v}$.

The tensors $\hat{\mathbf{G}}$ and $\hat{\mathbf{I}}$ are both symmetric, positive definite, and they commute with each other. As a result, they can be simultaneously diagonalized in the same reference system. The principal axes system, denoted as $\mathcal{S}^0$, is defined as the reference system with its origin at the center of mass, in which both tensors can be diagonalized. Let $\hat{\mathbf{e}}_\alpha$ with $\alpha = 1, 2, 3$ be the basis vectors of the inertial laboratory reference system $\mathcal{S}$ and $\hat{\mathbf{e}}^0_\alpha$ be the basis of the non-inertial principal axes reference system $\mathcal{S}^0$. The components of the rotation matrix of $\mathcal{S}^0$ with respect to $\mathcal{S}$ are defined as

$$\hat{\boldsymbol{\mathcal{R}}}_{\alpha\beta} = \hat{\mathbf{e}}^T_\beta \cdot \hat{\mathbf{e}}^0_\alpha \tag{3}$$

This shows that $\hat{\mathbf{e}}^0_\alpha$ are the *rows* of the rotation matrix $\boldsymbol{\mathcal{R}}$. In $\mathcal{S}^0$ the gyration and inertia tensor take the form

$$\begin{aligned} \hat{\boldsymbol{\mathcal{R}}} \cdot \hat{\mathbf{G}} \cdot \hat{\boldsymbol{\mathcal{R}}}^T &= \hat{\mathbb{G}} \\ \hat{\boldsymbol{\mathcal{R}}} \cdot \hat{\mathbf{I}} \cdot \hat{\boldsymbol{\mathcal{R}}}^T &= \hat{\mathbb{I}} \end{aligned} \tag{4}$$

where $\hat{\mathbb{G}}$ is a diagonal matrix whose elements are the central moments $\hat{M}_1, \hat{M}_2, \hat{M}_3$, which we write compactly as a list $\hat{\mathbf{M}} = (\hat{M}_1, \hat{M}_2, \hat{M}_3)$. Also, $\hat{\mathbb{I}}$ is a diagonal matrix whose elements are the principal moments $\hat{I}_1, \hat{I}_2, \hat{I}_3$. In this paper, diagonal matrices are represented with voided fonts, as in $\mathbb{A}$. As the inertia tensor (2) can be expressed in terms of the gyration tensor (1) in a linear way, the eigenvalues of the inertia tensor are given in terms of the eigenvalues of the gyration tensor as

$$\hat{I}_\alpha = 4\left(\hat{M}_1 + \hat{M}_2 + \hat{M}_3 - \hat{M}_\alpha\right) \tag{5}$$

Finally, observe that according to (4), the vectors $\hat{\mathbf{e}}^0_\alpha$ are the unit eigenvectors of the gyration and inertia tensors.

The rotation matrix can be expressed in terms of the exponential matrix

$$\hat{\boldsymbol{\mathcal{R}}} = e^{-[\hat{\boldsymbol{\Lambda}}]_\times} \tag{6}$$

where $\hat{\boldsymbol{\Lambda}}$ are the attitude parameters, or orientation for short. The angular velocity vector $\boldsymbol{\omega}$ is defined as [2, 8]

$$\frac{d}{dt}\boldsymbol{\mathcal{R}} \equiv -\boldsymbol{\mathcal{R}} \cdot [\boldsymbol{\omega}]_\times \tag{7}$$

The time derivative of the orientation and the angular velocity are related through [8]

$$\frac{d\boldsymbol{\Lambda}}{dt} = \mathbf{B} \cdot \boldsymbol{\omega} \tag{8}$$

where $\mathbf{B}$ is the Attitude Kinematic Operator [28] given by

$$\mathbf{B} = \mathbb{1} + p[\mathbf{n}]_\times + q[\mathbf{n}]_\times \cdot [\mathbf{n}]_\times \tag{9}$$

where $\mathbb{1}$ is the identity matrix, $\mathbf{n} = \boldsymbol{\Lambda}/\Lambda$ with $\Lambda = |\boldsymbol{\Lambda}|$, and p, q are the following functions of the modulus of the orientation Λ

$$p = -\frac{\Lambda}{2}, \qquad q = 1 - \frac{\Lambda}{2}\frac{\sin\Lambda}{(1-\cos\Lambda)} \tag{10}$$

From (4) and (6), the gyration tensor can be written as

$$\hat{\mathbf{G}} = e^{[\hat{\boldsymbol{\Lambda}}]_\times} \cdot \hat{\mathbb{G}} \cdot e^{-[\hat{\boldsymbol{\Lambda}}]_\times} \tag{11}$$

which can be understood as a change of variables from the six independent components of the symmetric gyration tensor, to the six degrees of freedom $\hat{\boldsymbol{\Lambda}}, \hat{\mathbf{M}}$. We have chosen in Ref. [8] the latter as the primary CG variables to describe the motion of a quasi-rigid free body.

The CG variables are phase functions, denoted with circumflexed symbols. As the microscopic state of the body evolves according to Hamilton's equations, the phase functions $\hat{\boldsymbol{\Lambda}}, \hat{\mathbf{M}}$ also evolve in time. The theory of CG offers a *modelling* of the evolution of the CG variables in terms of a diffusive Markov process. The corresponding Ito SDE for the orientation $\boldsymbol{\Lambda}$ is given by [8]

$$d\boldsymbol{\Lambda} = \mathbf{B} \cdot \left(\boldsymbol{\Omega} - \boldsymbol{\Gamma}^\wedge \cdot \mathbf{B}^{-T} \cdot (\boldsymbol{\Omega} \times \mathbf{S})\right) dt + k_B T \mathbf{F}^{\text{th}} dt + d\tilde{\boldsymbol{\Lambda}} \tag{12}$$

where the spin velocity $\mathbf{\Omega}$ is obtained from the conserved angular momentum $\mathbf{S}$ of the body as

$$\mathbf{\Omega} = \mathbf{I}^{-1} \cdot \mathbf{S} \tag{13}$$

The spin velocity $\mathbf{\Omega}$ is a dynamic quantity which is different from the angular velocity $\boldsymbol{\omega}$ introduced in (7) which is a purely kinematic quantity. For a rigid body both quantities coincide but for a real body they are different [8]. The dissipative matrix in (12) is given by

$$\mathbf{\Gamma}^{\Lambda} = \mathbf{B} \cdot e^{[\mathbf{\Lambda}]_\times} \cdot \boldsymbol{\mathcal{D}}_0 \cdot e^{-[\mathbf{\Lambda}]_\times} \cdot \mathbf{B}^T \tag{14}$$

where $\boldsymbol{\mathcal{D}}_0$ is the orientational diffusion matrix. This matrix is defined in terms of Green-Kubo formulae [8] and it is a symmetric and positive definite matrix by construction. In particular, it has a well-defined square root matrix.

The component α of the thermal drift vector $\mathbf{F}^{\rm th}$ is given in terms of the Kinematic Operator as (see Eq. (135) of [8])

$$\mathbf{F}^{\rm th}_\alpha = \left(\frac{\partial \mathbf{B}_{\alpha' \alpha}}{\partial \Lambda_\beta} \right) \boldsymbol{\mathcal{D}}_0^{\alpha' \beta'} \mathbf{B}_{\beta' \beta} \tag{15}$$

The noise term in (12) has the form

$$d\tilde{\mathbf{\Lambda}} = (2 k_B T)^{1/2} \mathbf{B} \cdot e^{[\mathbf{\Lambda}]_\times} \cdot \boldsymbol{\mathcal{D}}_0^{1/2} \cdot d\tilde{\mathbf{W}} \tag{16}$$

where $d\tilde{\mathbf{W}}$ is a vector of independent increments of the Wiener process satisfying the mnemotechnical Ito rule

$$d\tilde{\mathbf{W}} d\tilde{\mathbf{W}}^T = \mathbb{1} dt \tag{17}$$

and the square root matrix $\boldsymbol{\mathcal{D}}_0^{1/2}$ satisfies

$$\boldsymbol{\mathcal{D}}_0^{1/2} \cdot \left(\boldsymbol{\mathcal{D}}_0^{1/2} \right)^T = \boldsymbol{\mathcal{D}}_0 \tag{18}$$

Now, all the symbols appearing in the SDE (12) for the orientation are defined.

The SDEs for the central moments obtained in [8] are

$$\begin{aligned} d\mathbf{M} &= \mathbf{\Pi} dt \\ d\mathbf{\Pi} &= \boldsymbol{\mathcal{K}} dt - \mathbf{\Gamma} \cdot \boldsymbol{\nu} dt + d\tilde{\mathbf{\Pi}} \end{aligned} \tag{19}$$

Here $\mathbf{\Pi}$ is the dilational momentum, defined by the first equation as the time derivative of the central moments. The α component of the dilational force is defined as

$$\begin{aligned} \boldsymbol{\mathcal{K}}_\alpha = \mathbf{M}_{\underline{\alpha}} \Bigg(& \frac{1}{2} \boldsymbol{\nu}_{\underline{\alpha}}^2 + 2 \left(\mathbf{\Omega}_p^T \cdot \mathbf{\Omega}_p - \mathbf{\Omega}_{p\underline{\alpha}}^2 \right) \\ & + \frac{k_B T}{2 \mathbf{M}_{\underline{\alpha}}} - [\mathbf{\Sigma}^{-1}]_{\underline{\alpha}\beta} (\mathbf{M}_\beta - \mathbf{M}^{\rm rest}_\beta) \Bigg) \end{aligned} \tag{20}$$

Here, repeated indices are summed over except if they are underlined. The need of breaking this Einstein's summation convention arises from the fact that the central moments do not transform as a vector. The dilational velocity is $\boldsymbol{\nu}_\alpha = \mathbf{\Pi}_\alpha / \mathbf{M}_\alpha$ and the spin velocity in the principal axes frame is $\mathbf{\Omega}_p = e^{-[\mathbf{\Lambda}]_\times} \cdot \mathbf{\Omega}$. The elasticity matrix $\mathbf{\Sigma}$ is proportional to the covariance of central moments fluctuations, given by

$$\mathbf{\Sigma} = \frac{1}{k_B T} \left\langle (\hat{\mathbf{M}} - \mathbf{M}^{\rm rest}) (\hat{\mathbf{M}} - \mathbf{M}^{\rm rest})^T \right\rangle^{\mathcal{E}} \tag{21}$$

where $\langle \cdots \rangle^{\mathcal{E}}$ is an average with the rest microcanonical ensemble [8]. $\mathbf{M}^{\rm rest}$ is the average of the central moments with the rest microcanonical ensemble. We refer to the contribution to $\boldsymbol{\mathcal{K}}$ quadratic in $\boldsymbol{\nu}$ as the convective term, whose physical meaning has been discussed in [8]. The contribution quadratic in $\mathbf{\Omega}$ is referred to as the centrifugal term, and the last term involving the elasticity matrix $\mathbf{\Sigma}$ as the elastic term. Observe that the dilational momentum equation in (19) involves a dissipative force $-\mathbf{\Gamma} \cdot \boldsymbol{\nu}$ that is to be interpreted as a dilational friction, where $\mathbf{\Gamma}$ is a dilational friction matrix.

The temperature of the body T appearing in the SDE (12) and (19) depends in general on the thermal energy $\mathcal{E}$ of the body. For the solid bodies considered in this work, typically

$$T = \frac{\mathcal{E}}{C} \tag{22}$$

where the heat capacity is given by the Dulong-Petit law $C = 3 N k_B$, where N is the number of atoms of the body. The thermal energy is defined as

$$\mathcal{E} = E - K^{\rm rot} - K^{\rm dil} \tag{23}$$

where E is the total conserved energy of the body, the rotational kinetic energy is

$$K^{\rm rot} = \frac{1}{2} \mathbf{S} \cdot \mathbf{I}^{-1} \cdot \mathbf{S} \tag{24}$$

and the dilational kinetic energy is

$$K^{\rm dil} = \frac{1}{2} \mathbf{\Pi} \cdot \mathbb{G}^{-1} \cdot \mathbf{\Pi} \tag{25}$$

The SDE (12) for the orientation and the SDE (19) for central moments are coupled through different terms. For example, the spin velocity $\mathbf{\Omega}$ in the orientation equation (12) contains the inertia tensor $\mathbf{I}$ that depends on the central moments. Observe that, in principle, the orientational diffusion tensor $\boldsymbol{\mathcal{D}}_0 = \boldsymbol{\mathcal{D}}_0(\mathbf{M}, \mathcal{E})$ and it depends on the instantaneous value of the central moments $\mathbf{M}$ and the thermal energy $\mathcal{E}$ [8]. On the other hand the equation of the central moments (19) depends on the orientation through the centrifugal term quadratic in the spin velocity.

The SDEE governing orientation and shape of the body has been derived with the Theory of Coarse-Graining, which is, by construction, thermodynamically consistent. In particular, we have shown in Ref. [8] that the First

and Second Laws are satisfied.

III. THE SDE AT ZERO ANGULAR MOMENTUM

In this section, we show that when the angular momentum of the body vanishes, the theory in Ref [8] outlined in Sec. II characterizes the evolution of the principal axes as an anisotropic Brownian motion on the unit sphere. We offer a detailed description of anisotropic Brownian motion on the sphere in the Appendix VII.

A. The evolution of orientation

When the angular momentum vanishes, $\mathbf{S} = 0$, (12) with (98), reduces to the following Ito SDE

$$d\mathbf{\Lambda} = k_B T \mathbf{F}^{\text{th}} dt + \mathbf{B}^T \cdot \mathbf{C} \cdot d\tilde{\mathbf{W}} \tag{26}$$

where

$$\mathbf{C} \equiv (2k_B T)^{1/2} \boldsymbol{\mathcal{D}}_0^{1/2} \tag{27}$$

We wish to obtain the SDE governing the evolution of the principal axes or, equivalently, of the rotation matrix. This requires deriving an equation for $\boldsymbol{\mathcal{R}} = e^{-[\mathbf{\Lambda}]_\times}$ through Ito Calculus. Calculations vastly simplify by using the Stratonovich SDE corresponding to (26) and use of ordinary calculus. In Appendix VIII we show that the Stratonovich SDE corresponding to the Ito SDE (26) is

$$d\mathbf{\Lambda} = \mathbf{B}^T \cdot \mathbf{C} \circ d\tilde{\mathbf{W}} \tag{28}$$

From (28) and by using the chain rule in ordinary calculus, we show in Appendix IX that the SDE governing the rotation matrix is

$$d\boldsymbol{\mathcal{R}} = -\left[\mathbf{C} \circ d\mathbf{W}_t\right]_\times \cdot \boldsymbol{\mathcal{R}} \tag{29}$$

Therefore, the column vectors of the rotation matrix satisfy the Stratonovich SDE

$$d\mathbf{c}_\alpha = -\left[\mathbf{C} \circ d\mathbf{W}_t\right]_\times \cdot \mathbf{c}_\alpha \tag{30}$$

or in terms of the vector product

$$d\mathbf{c}_\alpha = \mathbf{c}_\alpha \times (\mathbf{C} \circ d\mathbf{W}_t) \tag{31}$$

This equation is identical to (54) in the Appendix VII that describes the anisotropic Brownian motion of a particle moving on the surface of a unit sphere. Therefore, the SDE (26) for the orientation predicts that the unit principal vectors describe an anisotropic Brownian motion on the sphere. It is straightforward to show that the SDEs (31) conserve the scalar products $\mathbf{c}_\alpha \cdot \mathbf{c}_\beta$ (see Appendix VII). Maintaining these conservation laws with a numerical integrator with finite time step requires special methods [27]. Instead of using (31), in the present paper we update the orientation $\mathbf{\Lambda}$ in (26) with a predictor-corrector scheme. This ensures automatically that the eigenvalues remain unitary at all times.

B. The evolution of the shape

Let us move now to the form of the SDE (19) for central moments when the angular momentum vanishes. In this case, the dilational force has no centrifugal component and (19) reduces to

$$\begin{aligned} d\mathbf{M}_\alpha &= \mathbf{\Pi}_\alpha dt \\ d\mathbf{\Pi}_\alpha &= \mathbf{M}_{\underline{\alpha}} \left(\frac{1}{2} \boldsymbol{\nu}_{\underline{\alpha}}^2 + \frac{k_B T}{2\mathbf{M}_{\underline{\alpha}}} - [\mathbf{\Sigma}^{-1}]_{\underline{\alpha}\beta} (\mathbf{M}_\beta - \mathbf{M}_\beta^{\text{rest}}) \right) dt \\ &\quad - \mathbf{\Gamma}_{\alpha\beta} \boldsymbol{\nu}_\beta dt + d\tilde{\mathbf{\Pi}}_\alpha \end{aligned} \tag{32}$$

Observe that when the body has zero angular momentum, the evolution of the central moments is uncoupled from the evolution of the orientation.

A good approximation to the set of equations (32) is given by the following linearized set of equations

$$\begin{aligned} d\mathbf{M}_\alpha &= \mathbf{\Pi}_\alpha dt \\ d\mathbf{\Pi}_\alpha &\simeq -\mathbf{M}_{\underline{\alpha}}^{\text{eq}} [\mathbf{\Sigma}^{-1}]_{\underline{\alpha}\beta} (\mathbf{M}_\beta - \mathbf{M}_\beta^{\text{rest}}) dt \\ &\quad - \mathbf{\Gamma}'_{\alpha\beta} \mathbf{\Pi}_\beta dt + d\tilde{\mathbf{\Pi}}_\alpha \end{aligned} \tag{33}$$

where we have approximated in some places $\mathbf{M} \simeq \mathbf{M}^{\text{eq}}$, have neglected the convective term quadratic in the dilational velocity $\boldsymbol{\nu}$ and the small term $k_B T / \mathbf{M}_\alpha$. Observe that when the angular momentum vanishes, we have $\mathbf{M}^{\text{eq}} = \mathbf{M}^{\text{rest}}$ by definition of $\mathbf{M}^{\text{rest}}$. Finally, we have redefined $\mathbf{\Gamma}'_{\alpha\beta} = \mathbf{\Gamma}_{\alpha\underline{\beta}} / \mathbf{M}_{\underline{\beta}}^{\text{eq}}$. With these approximations, the evolution of the central moments is an Ornstein-Uhlenbeck (OU) process, for which the equilibrium time-correlation of central moments can be explicitly computed. The equilibrium time correlation functions oscillate with frequencies determined by the elasticity matrix $\mathbf{\Sigma}$ which decay in a time scale determined by the dilational friction matrix $\mathbf{\Gamma}'$.

IV. EQUILIBRIUM MD SIMULATIONS AT $\mathbf{S} = 0$

In this section, we consider equilibrium MD simulations of a small body directed to measure the different parameters that enter the SDE (12), (19). These parameters will then be used in non-equilibrium simulations in order to validate the theory.

Simulations have been carried out with LAMMPS (Large-scale Atomic/Molecular Massively Parallel Simulator), where a parallelepiped crystal made of 6x5x3 atoms interacting with a Lennard-Jones potential (LJ) was constructed. Also, to ensure atomic cohesion, we add a non-linear bond contribution. Last, to maintain the crystal's shape, but to allow some deformation in

it, we add an angular potential. Details of the numerical simulations are given in the Supplemental Material (SM). We take ϵ, σ and m (the mass of one atom) as fundamental LJ units, so that $\tau = m\sigma^2/\epsilon$ is our unit of time. The initial microstate is selected by first carrying out an NVT simulation to equilibrate the crystal to a prescribed temperature T using a Nosé-Hoover thermostat. In order to average different simulations, we uniformly choose 30 equilibrated microstates and we subject each of them to a transformation leading to a fixed value E of the energy and to a zero value of the angular momentum vector. Then, each microscopic configuration evolves in an NVE ensemble until the system is fully equilibrated at the prescribed energy. Once we have a typical equilibrium state at energy E and zero angular momentum, we consider two types of simulations, equilibrium and non-equilibrium. In the equilibrium simulations we continue in the NVE ensemble to enter a production phase in which we measure different observables. In non-equilibrium simulations, we produce an angular kick that transforms the velocities in the initial typical equilibrium microstate in such a way that the system begins to rotate at a particular initial angular velocity around the intermediate principal axis. Details on the implementation of the angular kick are given in the Supplemental Material.

We set the total energy for the NVE simulations to $E = 2342\epsilon$. This value is a typical one observed in the NVT equilibration phase. Through the equipartion theorem [8]

$$\left\langle \sum_i \frac{m_i}{2} \mathbf{v}_i^2 \right\rangle_{\text{rest}}^{\mathcal{E}} = \frac{3(N-2)k_B T}{2} \tag{34}$$

this corresponds to a temperature of $T = 8.7\epsilon/k_B$. We have checked that, to a very good approximation the temperature scales linearly with the total energy, $E = CT$ with the heat capacity following the Dulong and Petit law $C = 3Nk_B$.

The gyration tensor $\hat{\mathbf{G}}(t)$ of the body as a function of time is computed from (1). The eigenvalues provide the central moments $\hat{\mathbf{M}}_\alpha(t)$ and the unit eigenvectors $\hat{\mathbf{e}}^0_\alpha(t)$ give the direction of the principal axes.

The measured equilibrium averages of the central moments at rest $\mathbf{M}^{\text{rest}}$ and the elasticity matrix $\mathbf{\Sigma}$ of the central moments (21) are

$$\begin{aligned} \mathbf{M}^{\text{rest}} &= (91.2, 62.5, 21.0) m\sigma^2 \\ \mathbf{\Sigma} &= \begin{pmatrix} 2.635 & 0.003 & 0.001 \\ 0.003 & 1.273 & 0.001 \\ 0.001 & 0.001 & 0.162 \end{pmatrix} \tau^4 \epsilon \end{aligned} \tag{35}$$

We have checked that the elasticity matrix is practically independent on the temperature in the range $T = 4 - 8$ in LJ units. Observe that the elasticity matrix is approximately diagonal. This entails a simplification in the dynamics of the central moments (33). By assuming that the dilational friction matrix $\mathbf{\Gamma}'$ is also diagonal, the evolution equations of the central moments (33) take the form (repeated indices are not summed over here)

$$\begin{aligned} d\mathbf{M}_\alpha &= \mathbf{\Pi}_\alpha dt \\ d\mathbf{\Pi}_\alpha &\simeq -\omega_\alpha^2 (\mathbf{M}_\alpha - \mathbf{M}_\alpha^{\text{rest}}) dt - \Gamma'_\alpha \mathbf{\Pi}_\alpha dt + d\tilde{\mathbf{\Pi}}_\alpha \end{aligned} \tag{36}$$

where $\omega_\alpha^2 = \mathbf{M}_\alpha^{\text{eq}} [\mathbf{\Sigma}^{-1}]_{\alpha\alpha}$ are the frequencies of oscillation. Using the values (35), the theoretical frequencies are

$$\omega_\alpha \to (5.873, 6.998, 11.363)\tau^{-1} \tag{37}$$

The equilibrium time-correlation for central moments, as predicted by the Ornstein-Uhlenbeck process is

$$\langle \mathbf{M}_\alpha(t) \mathbf{M}_\alpha \rangle^{\text{eq}} = \langle \mathbf{M}_\alpha \mathbf{M}_\alpha \rangle^{\text{eq}} e^{-\Gamma'_\alpha t} \cos(\omega_\alpha t) \tag{38}$$

In Fig. 2 we show the equilibrium time correlation functions for the central moments. To these curves, we have fitted the expressions (38) with the fitting parameters

$$\begin{aligned} \omega_\alpha &\to (5.870, 7.008, 11.357)\tau^{-1} \\ \mathbf{\Gamma}' &= \begin{pmatrix} 0.0295 & 0 & 0 \\ 0 & 0.0393 & 0 \\ 0 & 0 & 0.0930 \end{pmatrix} \tau^{-1} \end{aligned} \tag{39}$$

The agreement of the fitted values for ω_α and the predicted values (37) is very good, and shows that the modelling of the central moments with a simple O-U process is quite accurate and allows us to measure the dilational friction matrix $\mathbf{\Gamma}'$.

Let us move now to the dynamics of the unit eigenvectors. As shown in Fig 1, the unit eigenvectors trace a random trajectory as a consequence of thermal fluctuations. We claim that these MD trajectories can be modelled as realizations of a Brownian motion on the unit sphere. To confirm that this is the case and that, consequently, the theory presented describes well the observed microscopic dynamics of the orientation of the body, we compute the equilibrium time correlation matrix of the eigenvectors

$$\mathbf{E}(t) \equiv \left\langle \hat{\mathbf{e}}^0(t) \hat{\mathbf{e}}^{0T} \right\rangle^{\text{eq}} \tag{40}$$

As shown in the Appendix VII, a crucial analytical prediction of the SDE (31) is that the equilibrium time correlation matrix of the eigenvectors is

$$\mathbf{E}(t) = \frac{1}{3} e^{-\mathbf{A}t} \tag{41}$$

where $e^{-\mathbf{A}t}$ is the exponential matrix, and the matrix $\mathbf{A}$ is given by

$$\mathbf{A} \equiv \frac{1}{2} \left(\text{Tr}[\mathbf{D}] \mathbb{1} - \mathbf{D} \right) \tag{42}$$

Here, the matrix $\mathbf{D}$ is related to the noise amplitude

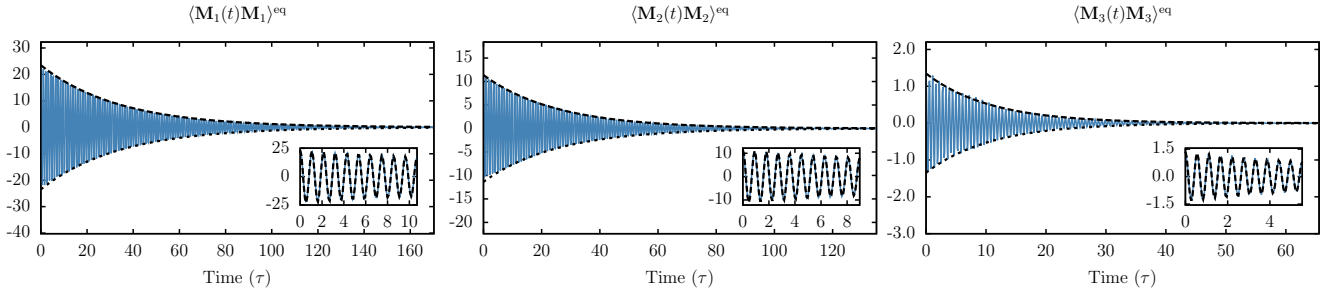

FIG. 2: The equilibrium time correlation function of the central moments $\langle \mathbf{M}_\alpha(t)\mathbf{M}_\alpha\rangle$ shows that the central moments display a damped oscillatory motion. From the maxima and minima of this curve we fit an exponential $e^{-\Gamma'_\alpha t}$ (in black) that allows us to extract the value of the dilational frictions Γ'_α. The insets show the fitting with (38).

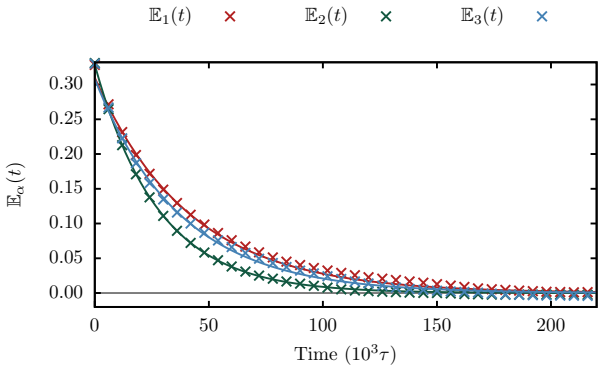

FIG. 3: The measured equilibrium autocorrelation functions $\mathbb{E}_\alpha(t)$ of the three principal eigenvectors as a function of time (symbols). Fitted to these curves are exponential functions (solid lines), from which the values $\mathbb{A}_\alpha$ are obtained using (45).

through

$$\mathbf{D} \equiv \mathbf{C}\cdot\mathbf{C}^T \overset{(27)}{=} 2k_BT\boldsymbol{\mathcal{D}}_0 \tag{43}$$

In terms of $\mathbf{A}$, $\boldsymbol{\mathcal{D}}_0$ is

$$\boldsymbol{\mathcal{D}}_0 = \frac{1}{k_BT}\left[\frac{1}{2}\mathrm{Tr}[\mathbf{A}]\mathbb{1} - \mathbf{A}\right] \tag{44}$$

as can be easily deduced by taking the trace of (42). The measured off-diagonal elements of the correlation matrix $\mathbf{E}(t)$ are vanishingly small. A diagonal time correlation matrix $\mathbf{E}(t) = \mathbb{E}(t)$ indicates that the matrix in (41) is also diagonal $\mathbf{A} = \mathbb{A}$. The autocorrelation function that resides in the diagonal of $\mathbf{E}(t)$ is predicted to decay as a simple exponential function

$$\begin{aligned}\mathbb{E}_1(t) &= \frac{1}{3}e^{-\mathbb{A}_1 t}\\ \mathbb{E}_2(t) &= \frac{1}{3}e^{-\mathbb{A}_2 t}\\ \mathbb{E}_3(t) &= \frac{1}{3}e^{-\mathbb{A}_3 t}\end{aligned} \tag{45}$$

We plot in Fig 3 the autocorrelation function of the principal unit vectors which decay exponentially, in full agreement with the theoretical prediction. From the fitting values for $\mathbb{A}_\alpha$ we extract the orientational diffusion matrix $\boldsymbol{\mathcal{D}}_0$, as follows. Because $\mathbf{A} = \mathbb{A}$ is diagonal (44) implies

$$\boldsymbol{\mathcal{D}}_0 = \frac{1}{k_BT}\left[\frac{1}{2}\mathrm{Tr}[\mathbb{A}]\mathbb{1} - \mathbb{A}\right] \tag{46}$$

which is a diagonal matrix. From the fitted values of $\mathbb{A}_\alpha$ in Fig. 3 the matrix takes the value

$$\boldsymbol{\mathcal{D}}_0 = \begin{pmatrix} 2.2338 & 0 & 0\\ 0 & 0.8587 & 0\\ 0 & 0 & 1.9129\end{pmatrix} \times 10^{-6}(\tau\epsilon)^{-1} \tag{47}$$

In summary, the exponential decay of the autocorrelation of unit eigenvalues allow us to measure the orientational diffusion matrix.

V. NON-EQUILIBRIUM SIMULATIONS WITH $\mathbf{S} \neq 0$

In this section, we will compare results from non-equilibrium microscopic MD simulations with non-equilibrium numerical solutions of the SDEs (26),(32) for a spinning body. The parameters to be used in the SDEs have been obtained in (35),(39),(47). Because the size of the system is small (the crystal has 90 atoms) thermal fluctuations are rather large and the signal to noise ratio is small. Therefore, in order to compare the noisy signals in both simulation methods, and to be able to validate the theory, it is necessary to perform some sort of averaging. On one hand, the average in the MD simulations will be over initial microstates compatible with a given (non-equilibrium) macrostate, i.e., with the same energy, angular momentum, and central moments. The first two observables (energy and angular momentum) are conserved by construction of the algorithm. To obtain microscopic configurations with the same value for the central moments $\mathbf{M}$, we carry out a long simulation in the NVE ensemble, compute the central moments along the entire simulation, and select those microstates which

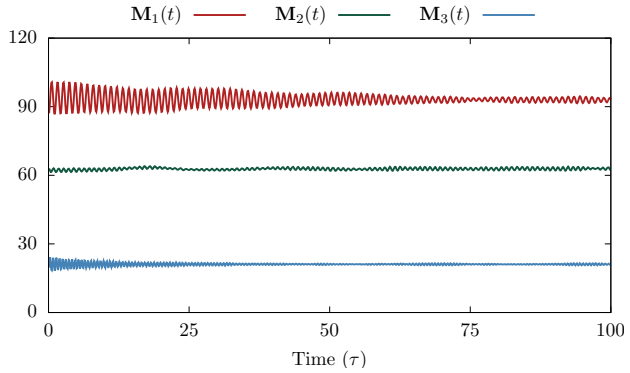

FIG. 4: Averaged central moments over 50 simulations, after the "angular kick". From top to bottom: M_1, M_2, and M_3. Observe that the central moment M_2 corresponding to the intermediate axis, is hardly affected by the centrifugal forces, while the decay time scales for M_1 and M_3 is different, reflecting different values of the dilational friction.

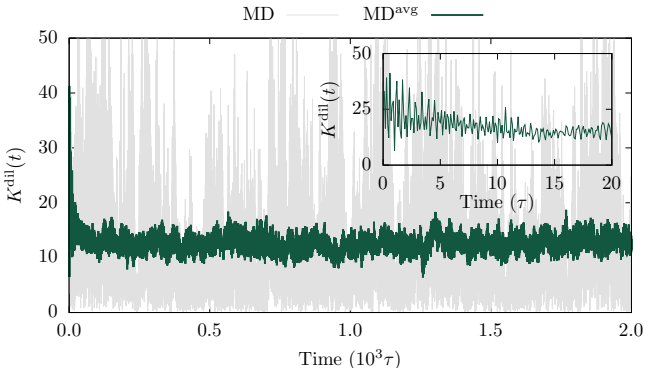

FIG. 5: Dilational energy $K^{\mathrm{dil}}(t)$ defined in (25) for an initial angular velocity $\Omega = 0.75\tau^{-1}$. Green line corresponds to the averaged value over 50 different initial conditions with the same value E, $\mathbf{S}$ and $\mathbf{M}$. Gray line corresponds to an individual MD simulation. Inset: zoom of the initial behavior of $K^{\mathrm{dil}}(t)$ that shows the decay of the dilational energy after the angular kick.

have similar values of $\mathbf{M}$. This is done through a Kmeans algorithm that cluster the central moments into groups of equal variance, minimizing the within-cluster sum-of-squares distance to the centroid of each group [30]. Following this procedure, we select a cluster of 50 different microscopic configurations with equal energy and angular momentum, and central moments differing by less than 1%. Note that we do not group the microstates with similar values of the dilational momenta $\mathbf{\Pi}$, which fluctuates around zero and seems to have no big effect on the results.

On the other hand, the average in the SDE will be done over different realizations of the stochastic process starting from an initial non-equilibrium macrostate identical to the one occurring in the MD simulations.

A. MD simulations

The non-equilibrium MD simulations are performed as follows. A microstate z is selected from the equilibrium simulations with prescribed values of $E, \mathbf{S}, \mathbf{M}$. Then, a rotation of the crystal is performed to reorient it with the intermediate axis in the y axis. This will enable us to observe the disappearance of the Dzhanibekov effect as a result of precession relaxation. Finally, an "angular kick" is imparted, as described in the Supplemental Material. This angular kick transforms the microstate z to z' with an angular velocity $\mathbf{\Omega} = (0, \Omega, 0)$ and the same original total energy E. We choose a value of $\Omega = 0.75\tau^{-1}$. If we run now the MD simulation starting from the new microstate z', the crystal will rotate around the intermediate axis with an angular momentum $\mathbf{S} = \mathbf{I} \cdot \mathbf{\Omega} \equiv \mathbf{S}^{\mathrm{eq}}$. After the applied angular kick, the centrifugal force produces an initial expansion of the crystal that starts oscillating, producing an oscillatory motion of the central moments which is superimposed to their thermal motion as shown in Fig. 4. Eventually these oscillations damp out and the dilational kinetic energy $K^{\mathrm{dil}}(t)$ defined in (25) goes down to its thermal noise level, as shown in Fig. 5. After the initial angular kick around the intermediate axis, the system rotates and displays the Dzhanibekov effect in very much the same way as in the fully deterministic case [16]. This effect is appreciable from the flip-flop evolution of the intermediate axis as shown in Fig. 6. At long times, due to precession relaxation the crystal ends up spinning around the major axis, which aligns with the conserved angular momentum vector. To keep track of the evolution of the system towards the equilibrium final state, we choose as observable the rotational kinetic energy $\hat{K}^{\mathrm{rot}}$ defined in (24). A single realization of the MD simulation is shown in gray in Fig 7, where it is apparent that the noise level does not allow for a clear distinction between signal and noise, thus justifying the averaging over 50 different simulations with the same E, $\mathbf{S}$ and similar central moments.

B. SDE simulations

We carried out 50 simulations of the SDEs with the same initial values of the orientation, central moments and dilational momenta of the corresponding non-equilibrium MD simulation, using a predictor-corrector explicit scheme[9]. In Fig. 7 we compare the average of the rotational kinetic energy K^{rot} obtained from the SDE (red) and MD (green) simulations. The rotational kinetic energy starts and ends at the same values in both SDE and MD, as a consequence of the identical initial macrostate selected. The stochastic precession relaxation produces a spinning about the major axis. The initial damping and long-term decay time of the MD signal is well captured by our SDE model. The very good agreement of the MD and SDE results provides a further validation of the proposed theory.

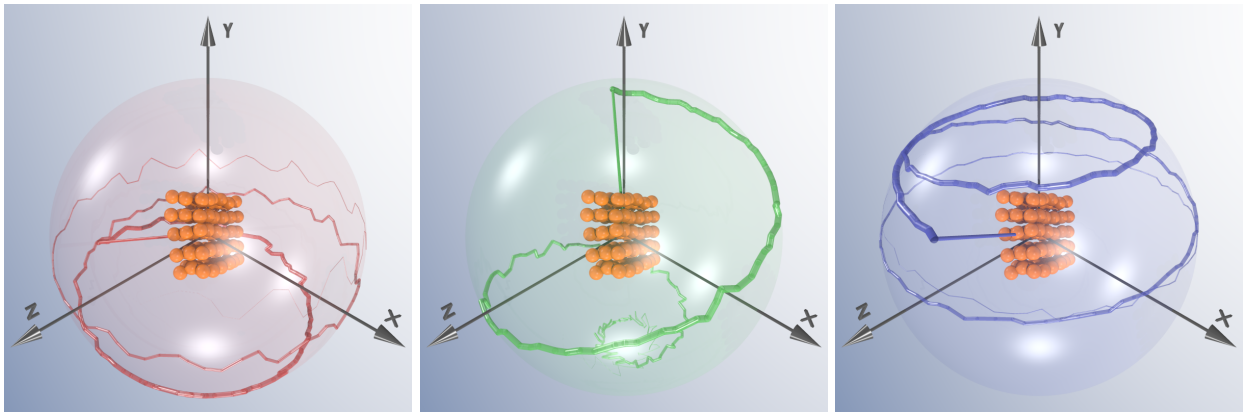

FIG. 6: Time evolution (plotted with increasing thickness) of the principal vectors $\mathbf{e}_1(t)$ (red, left), $\mathbf{e}_2(t)$ (green, middle), and $\mathbf{e}_3(t)$ (blue, right) for one particular MD simulation. The Dzhanibekov effect where $\mathbf{e}_2(t)$ flips direction is noticeable: at early times (thinner thickness of the line) $\mathbf{e}_2(t)$ is pointing downwards, and at later times (thicker thickness) it is pointing upwards. A video illustrating the process described above is provided as Supplementary Material.

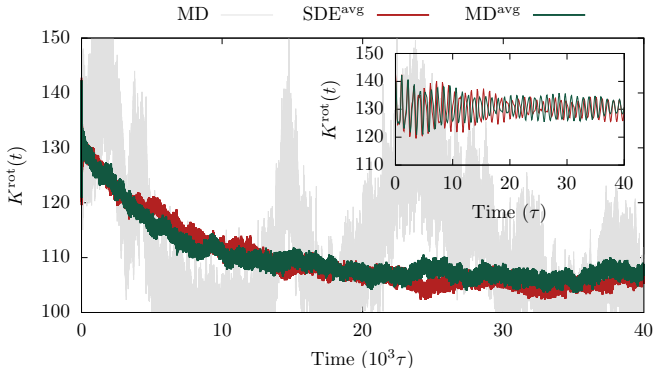

FIG. 7: Comparison of the average rotational kinetic energy $K^{\rm rot}(t)$ for an initial angular velocity $\Omega = 0.75\tau^{-1}$ and the same values of $E, \mathbf{S}, \mathbf{M}$. Red line corresponds to an average over 50 different realizations of the SDE simulations. Green line corresponds to the average over 50 initial conditions in MD simulations. Gray line corresponds to an individual MD simulation. Inset: Zoom of the initial behavior of $K^{\rm rot}(t)$ that captures the fact that the angular kick excites oscillatory motion of the central moments through centrifugal forces. This effect is also reproduced in the SDE simulations. The time scale of the initial oscillations in the inset coincides with the time scale of the damping of central moments at equilibrium, as shown in Figs. 1.

VI. CONCLUSIONS

In this paper we have compared the predictions of the Stochastic Dissipative Euler's Equations (12),(19) with the results of Molecular Dynamics simulation. Fitting parameters at equilibrium allows us to predict the non-equilibrium precession relaxation of the body, reflected in the evolution of the average rotational kinetic energy. In addition, when angular momentum vanishes, we confirm through the exponential decay of the autocorrelation function of the principal unit eigenvectors that the motion of these vectors can be modelled as an anisotropic Brownian motion, where the stochasticity is intrinsic, rather than due to an external bath (gas or liquid). The agreement between the theoretical model and the simulations is excellent, thus confirming the validity of the former.

We have observed that orientational diffusion strongly depends on the value of the rest central moments. Changing the size and geometry of the body changes strongly the value of the coefficients. Larger bodies display much smaller orientation fluctuations. In addition, the correlation time of the principal axes also depends strongly on the body's dimensions, increasing with size. As a consequence, MD simulations are readily unfeasible to access the long time scales in which a non-spinning body will change its overall orientation. In order to estimate the orientational diffusion coefficients from MD, we can only consider small bodies. We are currently attempting to find scaling relationship between geometry and the orientational diffusion coefficients. This requires extremely long simulation times, and will be presented elsewhere. On the other hand, using very small bodies (such as molecules) can result in Hamiltonian flows that are non-mixing, potentially leading to the absence of a well-defined equilibrium state. This poses a challenge, as a well-defined equilibrium is an implicit assumption in modeling mesoscopic dynamics with a diffusion Markov process. Not all interaction potentials between the particles of the body ensure the mixing property. For example, using almost linear harmonic springs does not give, in general, an ergodic system, as the famous Fermi-Pasta-Ulam-Tsingou problem of thermalization showed [31–34]. We have dealt with this problem by ensuring sufficiently non-linear interactions, based on the Lennard-Jones potential and adding strong non-linear bond interactions. The model atomic potential energy considered in the present paper does not correspond necessarily to a real material. Future work should focus on realistic potentials

for diamond and silica, for example. Further comparisons between theory and MD simulations are strongly constrained to a small window of system sizes: smaller sizes may not be ergodic, larger body sizes lead to extremely long correlation times. It is possible to play with temperature, as we have observed that orientational diffusion increases with the temperature of the body. In the present paper, in order to have observable effects that allow for a quantitative precise estimation of d_α we have considered very high temperatures ($k_B T \simeq 9\epsilon$) that may not be entirely realistic. Because the model selected does not correspond necessarily to a real material, we are not yet able to provide accurate estimates of the time scales involved in the precession relaxation rate for real materials of realistic sizes.

The present theory describes orientational diffusion due to intrinsic thermal fluctuations. The phenomena is very different from rotational diffusion due to the interaction with an ambient gas that produces additional friction. This latter phenomenon should be modelled with a Brownian rotor with viscous friction [23–27] or with kinetic theory [35]. For a dense gas, it is anticipated that the friction with the gas will dominate over the intrinsic orientational diffusion. It is an open question at which gas densities the intrinsic rotational diffusion, as discussed in this paper, will be surpassed by the effects of gas friction. Interaction with radiation as it is encountered in optolevitodynamic experiments is also a source of stochasticity due to the discrete nature of photons. The comparison of the magnitude of these different effects clearly deserves further study. The significance of the present work lies in its validation of the theoretical model by comparing it with Molecular Dynamics (MD) simulations in situations where such comparisons are feasible.

Acknowledgments

We thank Mark Thachuck for his useful comments regarding this manuscript. This research has been supported through MCIN grants PDC2021-121441-C22 and PID2020-117080RB-C54. JSR acknowledges the support of the Ministerio de Ciencia, Innovación y Universidades of Spain under a Margarita Salas contract funded by the European Union-NextGenerationEU. We acknowledge the computational resources and assistance provided by the Centro de Computación de Alto Rendimiento CCAR-UNED.

VII. APPENDIX: BROWNIAN MOTION ON A SPHERE

In this appendix, we summarize some mathematical results on the Brownian motion of a particle on the surface of a sphere and its anisotropic generalization.

A. Ito vs Stratonovich

We first recall the connection between the Ito and Stratonovich interpretation of an SDE. The following Ito SDE

$$d\mathbf{x} = \mathbf{A}(\mathbf{x})dt + \mathbf{\Theta}(\mathbf{x})\cdot d\mathbf{W}_t \tag{48}$$

with $\mathbf{A}(\mathbf{x})$ the drift, $\mathbf{\Theta}(\mathbf{x})$ the noise amplitude matrix, and $d\mathbf{W}_t$ a vector of independent increments of the Wiener process, corresponds to the following Stratonovich SDE [36]

$$d\mathbf{x} = \left[\mathbf{A}(\mathbf{x}) - \mathbf{V}(\mathbf{x})\right] dt + \mathbf{\Theta}(\mathbf{x}) \circ d\mathbf{W}_t \tag{49}$$

where the stochastic drift is

$$\mathbf{V}_i = \frac{1}{2}\mathbf{\Theta}_{kj}\frac{\partial}{\partial \mathbf{x}_k}\mathbf{\Theta}_{ij} \tag{50}$$

and repeated indices are summed over. Both SDE (48), (49) correspond to the following Fokker-Planck Equation (FPE)

$$\partial_t P(\mathbf{x},t) = -\frac{\partial}{\partial \mathbf{x}}\mathbf{A}P(\mathbf{x},t) + \frac{1}{2}\frac{\partial}{\partial \mathbf{x}}\frac{\partial}{\partial \mathbf{x}}\mathbf{\Theta}\mathbf{\Theta}^T P(\mathbf{x},t) \tag{51}$$

B. Anisotropic Brownian motion on the sphere

It is well-known [21, 22] that the evolution of a particle with position $\mathbf{r} \in \mathbb{R}^3$ on the surface of a sphere due to Brownian motion is described by the following Stochastic Differential Equation (SDE)

$$d\mathbf{r} = [\mathbf{r}]_\times \circ d\mathbf{W}_t \qquad \text{Stratonovich} \tag{52}$$

with the corresponding SDE in the Ito interpretation

$$d\mathbf{r} = -\mathbf{r} + [\mathbf{r}]_\times \cdot d\mathbf{W}_t \qquad \text{Ito} \tag{53}$$

where $d\mathbf{W}_t \in \mathbb{R}^3$ is a a vector of independent increments of the Wiener process and $[\mathbf{r}]_\times$ is the cross-product matrix formed from the vector $\mathbf{r}$.

A natural generalization of the SDE (52) for describing *non-isotropic* Brownian motion on the sphere is

$$d\mathbf{r} = [\mathbf{r}]_\times \cdot \mathbf{C} \circ d\mathbf{W}_t \qquad \text{Stratonovich} \tag{54}$$

where $\mathbf{C} \in \mathbb{R}^{3\times 3}$ is a constant symmetric matrix. We write this equation in the form (49)

$$d\mathbf{r} = \mathbf{\Theta}(\mathbf{r}) \circ d\mathbf{W}_t \tag{55}$$

where

$$\mathbf{\Theta}(\mathbf{r}) = [\mathbf{r}]_\times \cdot \mathbf{C} \tag{56}$$

and $\mathbf{C}$ is a constant matrix. The corresponding Ito SDE

is given by

$$d\mathbf{r} = \mathbf{V}dt + \mathbf{\Theta}\cdot d\mathbf{W}_t \tag{57}$$

where $\mathbf{V}$ is given in (50). Noting that the matrix $\mathbf{\Theta}$ has components

$$\mathbf{\Theta}_{ij} = \epsilon_{ilm}\mathbf{r}_l\mathbf{C}_{mj} \tag{58}$$

then

$$\begin{aligned}\mathbf{V}_i(\mathbf{x}) &= \frac{1}{2}\mathbf{\Theta}_{kj}\frac{\partial}{\partial \mathbf{r}_k}\mathbf{\Theta}_{ij} \\ &= \frac{1}{2}\epsilon_{kl'm'}\mathbf{r}_{l'}\mathbf{C}_{m'j}\frac{\partial}{\partial \mathbf{r}_k}\epsilon_{ilm}\mathbf{r}_l\mathbf{C}_{mj} \\ &= -\frac{1}{2}\left(\mathrm{Tr}[\mathbf{C}\cdot\mathbf{C}^T]\mathbf{r}_i - \mathbf{C}_{ij}\mathbf{C}_{mj}\mathbf{r}_m\right)\end{aligned} \tag{59}$$

which means

$$\mathbf{V} = -\frac{1}{2}\left(\mathrm{Tr}[\mathbf{D}]\mathbb{1} - \mathbf{D}\right)\cdot\mathbf{r}, \tag{60}$$

where we have defined the symmetric positive definite diffusion tensor

$$\mathbf{D} \equiv \mathbf{C}\cdot\mathbf{C}^T \tag{61}$$

and the superscript T denotes the transpose matrix. The Ito SDE (57) is then

$$d\mathbf{r} = -\mathbf{A}\cdot\mathbf{r} + [\mathbf{r}]_\times\cdot\mathbf{C}\cdot d\mathbf{W}_t \qquad \text{Ito} \tag{62}$$

where the matrix $\mathbf{A} \in \mathbb{R}^{3\times 3}$ is

$$\mathbf{A} \equiv \frac{1}{2}\left(\mathrm{Tr}[\mathbf{D}]\mathbb{1} - \mathbf{D}\right) \tag{63}$$

Here $\mathbb{1}$ is the unit matrix. The matrix $\mathbf{A}$ is symmetric and positive definite. This can be easily seen from the fact that $\mathbf{A}, \mathbf{D}$ commute and, hence diagonalize in the same basis. If the eigenvalues of $\mathbf{D}$ are (d_1, d_2, d_3), then the eigenvalues of $\mathbf{A}$ are easily seen to be $\left(\frac{d_2+d_3}{2}, \frac{d_2+d_3}{2}, \frac{d_1+d_2}{2}\right)$. Because $d_\alpha > 0$, all the eigenvalues of $\mathbf{A}$ are positive. When $\mathbf{C} = \mathbb{1} = \mathbf{D}$, then $\mathbf{A} = \mathbb{1}$, and (54) recovers the SDE (52) for isotropic Brownian motion.

C. The FPE for anisotropic Brownian motion

To get the FPE that corresponds to the Ito SDE (62) we translate the connection between the FPE (51) and the Ito SDE (48), this is

$$\begin{aligned}\partial_t P(\mathbf{r},t) &= \frac{\partial}{\partial \mathbf{r}}\left[\frac{1}{2}\left(\mathrm{Tr}[\mathbf{D}]\mathbb{1} - \mathbf{D}\right)\cdot\mathbf{r}\right]P(\mathbf{r},t) + \frac{1}{2}\frac{\partial}{\partial \mathbf{r}}\frac{\partial}{\partial \mathbf{r}}[\mathbf{r}]_\times\cdot\mathbf{C}\cdot\mathbf{C}^T[\mathbf{r}]_\times^T P(\mathbf{r},t) \\ &= \frac{\partial}{\partial \mathbf{r}}\left[\frac{1}{2}\left(\mathrm{Tr}[\mathbf{D}]\mathbb{1} - \mathbf{D}\right)\cdot\mathbf{r}\right]P(\mathbf{r},t) + \frac{1}{2}\frac{\partial}{\partial \mathbf{r}}[\mathbf{r}]_\times\cdot\mathbf{D}\cdot[\mathbf{r}]_\times^T\frac{\partial}{\partial \mathbf{r}}P(\mathbf{r},t) + \frac{1}{2}\frac{\partial}{\partial \mathbf{r}}\left(\frac{\partial}{\partial \mathbf{r}}[\mathbf{r}]_\times\cdot\mathbf{D}\cdot[\mathbf{r}]_\times^T\right)P(\mathbf{r},t)\end{aligned} \tag{64}$$

Let us compute the term within rounded parenthesis

$$\begin{aligned}\left(\frac{\partial}{\partial \mathbf{r}_j}\left[[\mathbf{r}]_\times\cdot\mathbf{D}\cdot[\mathbf{r}]_\times^T\right]_{ij}\right) &= -\frac{\partial}{\partial \mathbf{r}_j}\epsilon_{iki'}\mathbf{D}_{i'j'}\epsilon_{j'k'j}\frac{\partial}{\partial \mathbf{r}_j}\mathbf{r}_k\mathbf{r}_{k'} = -\epsilon_{iki'}\epsilon_{j'k'j}\mathbf{D}_{i'j'}\left(\delta_{kj}\mathbf{r}_{k'} + \delta_{k'j}\mathbf{r}_k\right) \\ &= -\epsilon_{iji'}\epsilon_{j'k'j}\mathbf{D}_{i'j'}\mathbf{r}_{k'} - \epsilon_{iki'}\underbrace{\epsilon_{j'jj}}_{=0}\mathbf{D}_{i'j'}\mathbf{r}_k \\ &= \epsilon_{ii'j}\epsilon_{j'k'j}\mathbf{D}_{i'j'}\mathbf{r}_{k'} = \left[\delta_{ij'}\delta_{i'k'} - \delta_{ik'}\delta_{i'j'}\right]\mathbf{D}_{i'j'}\mathbf{r}_{k'} = \delta_{ij'}\delta_{i'k'}\mathbf{D}_{i'j'}\mathbf{r}_{k'} - \delta_{ik'}\delta_{i'j'}\mathbf{D}_{i'j'}\mathbf{r}_{k'} \\ &= \mathbf{D}_{i'i}\mathbf{r}_{i'} - \mathrm{Tr}[\mathbf{D}]\mathbf{r}_i\end{aligned} \tag{65}$$

The last term in the rhs of (64) then cancels the first term and the FPE (64) for anisotropic Brownian motion is simply

$$\partial_t P(\mathbf{r},t) = \frac{1}{2}\frac{\partial}{\partial \mathbf{r}}[\mathbf{r}]_\times^T\cdot\mathbf{D}\cdot[\mathbf{r}]_\times\frac{\partial}{\partial \mathbf{r}}P(\mathbf{r},t) \tag{66}$$

The diffusion matrix of this FPE is clearly positive (semi) definite, because, for any arbitrary vector $\mathbf{v}$ we have

$$\begin{aligned}\mathbf{v}^T\cdot[\mathbf{r}]_\times^T\cdot\mathbf{D}\cdot[\mathbf{r}]_\times\cdot\mathbf{v} &= \mathbf{v}^T\cdot[\mathbf{r}]_\times^T\cdot\mathbf{C}\cdot\mathbf{C}^T\cdot[\mathbf{r}]_\times\cdot\mathbf{v} \\ &= \left(\mathbf{C}^T\cdot[\mathbf{r}]_\times\cdot\mathbf{v}\right)^2 \geq 0\end{aligned} \tag{67}$$

D. The equilibrium distribution for spherical Brownian motion

Let us find the equilibrium distribution of the FPE (66). Observe that any probability of the form $P(\mathbf{r}) = \phi(r)$, with $r = |\mathbf{r}|$, is a stationary solution of the FPE (66) because

$$\frac{\partial}{\partial \mathbf{r}}\phi(r) = \phi'(r)\frac{\mathbf{r}}{r} \tag{68}$$

At the same time, any average of a function $F(r)$ is time-independent. This is shown as follows

$$\begin{aligned}
&\frac{d}{dt}\int d\mathbf{r}F(r)P(\mathbf{r},t)\\
&= \int d\mathbf{r}F(r)\frac{1}{2}\frac{\partial}{\partial \mathbf{r}}\cdot[\mathbf{r}]_\times^T\cdot\mathbf{D}\cdot[\mathbf{r}]_\times\frac{\partial}{\partial \mathbf{r}}P(\mathbf{r},t)\\
&= -\frac{1}{2}\int d\mathbf{r}\frac{\partial F(r)}{\partial \mathbf{r}}\cdot[\mathbf{r}]_\times^T\cdot\mathbf{D}\cdot[\mathbf{r}]_\times\frac{\partial}{\partial \mathbf{r}}P(\mathbf{r},t) = 0\\
&= -\frac{1}{2}\int d\mathbf{r}F'(r)\underbrace{\frac{\mathbf{r}}{r}\cdot[\mathbf{r}]_\times^T}_{=0}\cdot\mathbf{D}\cdot[\mathbf{r}]_\times\frac{\partial}{\partial \mathbf{r}}P(\mathbf{r},t) = 0
\end{aligned} \tag{69}$$

Now consider the probability that the particle has a particular modulus r. By definition it is given by the push-forward

$$P(r,t) = \int d\mathbf{r}\delta(r-|\mathbf{r}|)P(\mathbf{r},t) \tag{70}$$

This quantity is, in fact, time-independent. It takes the value $P(r,0)$ that it has at the initial time and, also, the value $P(r,\infty) = P(r,0)$ that has at equilibrium. Therefore, we have

$$\begin{aligned}
P(r,0) &= \int d\mathbf{r}\delta(r-|\mathbf{r}|)P^{\rm eq}(\mathbf{r})\\
&= \phi(r)\int d\mathbf{r}\delta(r-|\mathbf{r}|) = \phi(r)4\pi r^2
\end{aligned} \tag{71}$$

This means that the equilibrium solution must be given by

$$P^{\rm eq}(\mathbf{r}) = \frac{P(r,0)}{4\pi r^2} \tag{72}$$

Observe that the stationary solution of the FPE depends on the initial distribution. For example, if the initial condition is one in which we are certain that the particle is at a particular point $\mathbf{r}_0$ on the surface of the unit sphere, i.e. $|\mathbf{r}_0| = 1$, the initial condition is $P(\mathbf{r},0) = \delta(\mathbf{r}-\mathbf{r}_0)$. The corresponding stationary solution of the FPE with this initial condition is

$$P^{\rm eq}(\mathbf{r}) = \frac{\delta(|\mathbf{r}|-1)}{4\pi} \tag{73}$$

E. Correlation function

The equilibrium correlation function of the position of a particle perfoming a Brownian motion on the unit sphere can be analytically computed, as follows. The FPE (66) can be written as

$$\partial_t P(\mathbf{r},t) = \mathcal{L}P(\mathbf{r},t) \tag{74}$$

where the Fokker-Planck operator is given by

$$\mathcal{L} = \frac{1}{2}\frac{\partial}{\partial \mathbf{r}}[\mathbf{r}]_\times^T\cdot\mathbf{D}\cdot[\mathbf{r}]_\times\frac{\partial}{\partial \mathbf{r}} \tag{75}$$

The stationary correlation function can be expressed as [37]

$$\langle \mathbf{r}_\alpha(t)\mathbf{r}_\beta\rangle = \int d\mathbf{r}P^{\rm eq}(\mathbf{r})\mathbf{r}_\beta e^{\mathcal{L}t}\mathbf{r}_\alpha \tag{76}$$

where the exponential of the Fokker-Planck operator is defined in terms of its series expansion

$$e^{\mathcal{L}t} = \sum_{n=0}^{\infty}\frac{t^n}{n!}\mathcal{L}^n \tag{77}$$

We wish to compute the action of the exponential operator on the unit vector, $e^{\mathcal{L}t}\mathbf{r}$. The second term in the series expansion is $\mathcal{L}\mathbf{r}$ that we write explicitly in component form as

$$\begin{aligned}
\mathcal{L}\mathbf{r}_\gamma &= -\frac{1}{2}\frac{\partial}{\partial \mathbf{r}_\mu}\epsilon_{\mu\alpha\mu'}\mathbf{r}_\alpha\mathbf{D}_{\mu'\nu'}\epsilon_{\nu'\beta\nu}\mathbf{r}_\beta\frac{\partial}{\partial \mathbf{r}_\nu}\mathbf{r}_\gamma\\
&= \frac{1}{2}\mathbf{D}_{\mu'\nu'}\epsilon_{\mu\alpha\mu'}\epsilon_{\mu\nu'\gamma}\mathbf{r}_\alpha\\
&= \frac{1}{2}\mathbf{D}_{\mu'\nu'}\left(\delta_{\alpha\nu'}\delta_{\mu'\gamma}-\delta_{\alpha\gamma}\delta_{\mu'\nu'}\right)\mathbf{r}_\alpha\\
&= \frac{1}{2}\mathbf{D}_{\gamma\alpha}\mathbf{r}_\alpha - \frac{1}{2}{\rm Tr}[\mathbf{D}]\mathbf{r}_\gamma
\end{aligned} \tag{78}$$

Therefore,

$$\mathcal{L}\mathbf{r} = -\mathbf{A}\cdot\mathbf{r} \tag{79}$$

where the matrix $\mathbf{A}$ has been defined in (63). It is then obvious that

$$e^{\mathcal{L}t}\mathbf{r} = e^{-\mathbf{A}t}\cdot\mathbf{r} \tag{80}$$

where the matrix exponential is introduced through the series expansion.

The correlation matrix (76) is now

$$\begin{aligned}
\langle \mathbf{r}_\alpha(t)\mathbf{r}_\beta\rangle &= \int d\mathbf{r}P^{\rm eq}(\mathbf{r})\mathbf{r}_\alpha\left[e^{-\mathbf{A}t}\right]_{\beta\beta'}\mathbf{r}_{\beta'}\\
&= \left[e^{-\mathbf{A}t}\right]_{\beta\beta'}\int d\mathbf{r}P^{\rm eq}(\mathbf{r})\mathbf{r}_\alpha\mathbf{r}_{\beta'}\\
&\overset{(73)}{=} \left[e^{-\mathbf{A}t}\right]_{\beta\beta'}\frac{1}{3}\delta_{\alpha\beta'}
\end{aligned} \tag{81}$$

and we conclude that the equilibrium time correlation matrix of the position of the Brownian particle on the unit sphere is given by

$$\left\langle \mathbf{r}(t)\mathbf{r}^T \right\rangle = \frac{1}{3} e^{-\mathbf{A}t} \tag{82}$$

F. Representation in terms of a rotation matrix

We consider now a time-dependent rotation matrix $\boldsymbol{\mathcal{R}}$

$$\boldsymbol{\mathcal{R}} = \left(\mathbf{c}_1, \mathbf{c}_2, \mathbf{c}_3 \right) \tag{83}$$

where $\mathbf{c}_\alpha$ are column vectors. Because $\boldsymbol{\mathcal{R}}$ is an orthogonal matrix, its columns $\mathbf{c}_\alpha$ form an orthonormal basis set. We propose now a SDE for the rotation matrix in such a way that the basis vectors describe a Brownian motion on the unit sphere. In order to reach this goal, we introduce the angular velocity $\boldsymbol{\omega}_0$ in the principal axes frame through

$$\frac{d}{dt}\boldsymbol{\mathcal{R}} \equiv -[\boldsymbol{\omega}_0]_\times \cdot \boldsymbol{\mathcal{R}} \tag{84}$$

to be compared with (7). Both angular velocities (7) and (84) are related through

$$\boldsymbol{\omega}_0 = \boldsymbol{\mathcal{R}} \cdot \boldsymbol{\omega} \tag{85}$$

We may use (84) as an *inspiration* to construct an SDE in the space of rotation matrices. To achieve this objective, we transform the angular velocity $\boldsymbol{\omega}_0$ into a stochastic process, this is

$$\boldsymbol{\omega}_0 \to \mathbf{C} \circ \frac{d\mathbf{W}_t}{dt} \tag{86}$$

and *postulate* the following Stratonovich SDE for the rotation matrix

$$d\boldsymbol{\mathcal{R}} = -\left[\mathbf{C} \circ d\mathbf{W}_t\right]_\times \cdot \boldsymbol{\mathcal{R}} \qquad \text{Stratonovich} \tag{87}$$

In terms of the columns $\mathbf{c}_\alpha$, we may write (87) in the form

$$\begin{aligned} d\mathbf{c}_1 &= -\left[\mathbf{C} \circ d\mathbf{W}_t\right]_\times \cdot \mathbf{c}_1 \\ d\mathbf{c}_2 &= -\left[\mathbf{C} \circ d\mathbf{W}_t\right]_\times \cdot \mathbf{c}_2 \\ d\mathbf{c}_3 &= -\left[\mathbf{C} \circ d\mathbf{W}_t\right]_\times \cdot \mathbf{c}_3 \end{aligned} \tag{88}$$

where in each equation we have exactly the same value of the independent increment of the Wiener process $d\mathbf{W}_t$. Therefore, the columns of the rotation matrix experience an anisotropic Brownian motion on the surface of the unit sphere of the form (54). We conclude that the postulated SDE (87) for the rotation matrix is an alternative representation of anisotropic Brownian motion.

Observe that the SDE (88) has a number of conserved quantities. By scalarly multiplying with $\mathbf{c}_\alpha$ we have

$$\mathbf{c}_\alpha^T \cdot d\mathbf{c}_\beta = \mathbf{c}_\alpha^T \cdot (\mathbf{c}_\beta \times \mathbf{C} \circ d\mathbf{W}_t) = (\mathbf{c}_\alpha \times \mathbf{c}_\beta)^T \cdot \mathbf{C} \circ d\mathbf{W}_t \tag{89}$$

and this implies

$$\begin{aligned} d(\mathbf{c}_\alpha^T \cdot \mathbf{c}_\beta) &= \mathbf{c}_\alpha^T \cdot d\mathbf{c}_\beta + \mathbf{c}_\beta^T \cdot d\mathbf{c}_\alpha \\ &= (\mathbf{c}_\alpha \times \mathbf{c}_\beta)^T \cdot \mathbf{C} \circ d\mathbf{W}_t + (\mathbf{c}_\beta \times \mathbf{c}_\alpha)^T \cdot \mathbf{C} \circ d\mathbf{W}_t = 0 \end{aligned} \tag{90}$$

This means that both the modulus of the vectors and the angle between them are conserved by the dynamics. If initially $\mathbf{c}_\alpha^T \cdot \mathbf{c}_\beta = \delta_{\alpha\beta}$, these orthonormality conditions are mantained at all times, as expected.

For future reference, we also construct the Ito version of the Stratonovich SDE 88). By analogy with (54), (62), the Stratonovich SDE (88) is equivalent to the following Ito SDE

$$d\mathbf{c}_\alpha = -\mathbf{A} \cdot \mathbf{c}_\alpha - [\mathbf{C} \cdot d\mathbf{W}]_\times \cdot \mathbf{c}_\alpha \tag{91}$$

where $\mathbf{A}$ is given by (63). Equation (91) is equivalent to the following Ito SDE for the rotation matrix

$$d\boldsymbol{\mathcal{R}} = -\mathbf{A} \cdot \boldsymbol{\mathcal{R}} - [\mathbf{C} \cdot d\mathbf{W}]_\times \cdot \boldsymbol{\mathcal{R}} \qquad \text{Ito} \tag{92}$$

This concludes our review of the anisotropic Brownian motion of a particle on the unit sphere.

VIII. APPENDIX: DERIVATION OF (28)

We start from the Stratonovich SDE (26) for the orientation

$$d\boldsymbol{\Lambda} = k_B T \mathbf{F}^{\text{th}} dt + \mathbf{B}^T \cdot \mathbf{C} \cdot d\tilde{\mathbf{W}} \tag{93}$$

where

$$\mathbf{C} \equiv (2k_B T)^{1/2} \boldsymbol{\mathcal{D}}_0^{1/2} \tag{94}$$

This is of the form of the Ito SDE (48) with

$$\begin{aligned} \mathbf{A} &= k_B T \mathbf{F}^{\text{th}} \\ \boldsymbol{\Theta} &= \mathbf{B}^T \cdot (2k_B T)^{1/2} \boldsymbol{\mathcal{D}}_0^{1/2} \end{aligned} \tag{95}$$

The corresponidng Stratonovich SDE (49) is now

$$d\boldsymbol{\Lambda} = \left(k_B T \mathbf{F}^{\text{th}} - \mathbf{V}\right) dt + \mathbf{B}^T \cdot \mathbf{C} \cdot \circ d\tilde{\mathbf{W}} \tag{96}$$

where the stochastic drift $\mathbf{V}$ is given by (50), which in the present case is

$$\begin{aligned} \mathbf{V}_i &= k_B T \left[\mathbf{B} \cdot \boldsymbol{\mathcal{R}}^T \cdot \boldsymbol{\mathcal{D}}_0^{1/2}\right]_{kj} \frac{\partial}{\partial \Lambda_k} \left[\mathbf{B} \cdot \boldsymbol{\mathcal{R}}^T \cdot \boldsymbol{\mathcal{D}}_0^{1/2}\right]_{ij} \\ &= k_B T \left[\mathbf{B} \cdot \boldsymbol{\mathcal{R}}^T\right]_{kk'} \left[\boldsymbol{\mathcal{D}}_0\right]_{k'i'} \frac{\partial}{\partial \Lambda_k} \left[\mathbf{B} \cdot \boldsymbol{\mathcal{R}}^T\right]_{ii'} \end{aligned} \tag{97}$$

The rotation matrix and the kinematic operator satisfy

$$\mathbf{B}\cdot\boldsymbol{\mathcal{R}}^T=\mathbf{B}^T \tag{98}$$

as can be shown from the results in Sec. K.1 of the Supplemental Material of Ref. [8]. By using the property (98), (97) becomes

$$\mathbf{V}_i=k_BT\left[\boldsymbol{\mathcal{D}}_0\right]_{k'i'}\mathbf{B}_{k'k}\frac{\partial}{\partial\Lambda_k}\mathbf{B}_{i'i}\overset{(15)}{=}k_BT\mathbf{F}_i^{\text{th}} \tag{99}$$

Therefore, (96) becomes

$$d\boldsymbol{\Lambda}=\mathbf{B}^T\cdot\mathbf{C}\circ d\tilde{\mathbf{W}} \tag{100}$$

which is (28), as we wished to demonstrate.

IX. APPENDIX: DERIVATION OF (29)

By using the chain rule of ordinary calculus with the Stratonovich SDE (28) we wish to obtain a Stratonovich SDE for the rotation matrix. Indeed

$$d\boldsymbol{\mathcal{R}}=\frac{\partial\boldsymbol{\mathcal{R}}}{\partial\boldsymbol{\Lambda}}\cdot d\boldsymbol{\Lambda}\overset{(28)}{=}\frac{\partial\boldsymbol{\mathcal{R}}}{\partial\boldsymbol{\Lambda}}\cdot\mathbf{B}^T\cdot\mathbf{C}\circ d\tilde{\mathbf{W}} \tag{101}$$

From the results in Sec. K.1 of the Supplemental Material of Ref. [8], the derivative of the rotation matrix with respect to the orientation is given by

$$\frac{\partial\boldsymbol{\mathcal{R}}_{\mu\nu}}{\partial\boldsymbol{\Lambda}_\alpha}=-\mathbf{B}^{-1}_{\alpha\beta}\epsilon_{\mu\beta\delta}\boldsymbol{\mathcal{R}}_{\delta\nu} \tag{102}$$

Using this derivative in (101) leads to

$$\begin{aligned}d\boldsymbol{\mathcal{R}}_{\mu\nu}&=\frac{\partial\boldsymbol{\mathcal{R}}_{\mu\nu}}{\partial\boldsymbol{\Lambda}_\alpha}\mathbf{B}_{\alpha\alpha'}\boldsymbol{\mathcal{R}}^T_{\alpha'\beta}[\mathbf{C}\cdot d\tilde{\mathbf{W}}_t]_\beta\\&=-\mathbf{B}^{-1}_{\alpha\beta}\epsilon_{\mu\beta\delta}\boldsymbol{\mathcal{R}}_{\delta\nu}\mathbf{B}_{\alpha\alpha'}\boldsymbol{\mathcal{R}}^T_{\alpha'\beta'}[\mathbf{C}\cdot d\tilde{\mathbf{W}}_t]_{\beta'}\\&=-\epsilon_{\mu\beta\delta}\boldsymbol{\mathcal{R}}_{\delta\nu}\underbrace{\mathbf{B}^{-1}_{\alpha\beta}\mathbf{B}_{\alpha\alpha'}\boldsymbol{\mathcal{R}}^T_{\alpha'\beta'}}_{[\mathbf{B}^{-T}\cdot\mathbf{B}\cdot\boldsymbol{\mathcal{R}}^T]_{\beta\beta'}}[\mathbf{C}\cdot d\tilde{\mathbf{W}}_t]_{\beta'}\end{aligned} \tag{103}$$

The property (98) implies

$$\mathbf{B}^{-T}\cdot\mathbf{B}\cdot\boldsymbol{\mathcal{R}}^T=\mathbb{1} \tag{104}$$

and, therefore,

$$\begin{aligned}d\boldsymbol{\mathcal{R}}_{\mu\nu}&=-\epsilon_{\mu\beta\delta}\boldsymbol{\mathcal{R}}_{\delta\nu}\underbrace{\mathbf{B}^{-1}_{\alpha\beta}\mathbf{B}_{\alpha\alpha'}\boldsymbol{\mathcal{R}}^T_{\alpha'\beta'}}_{\delta_{\beta\beta'}}[\mathbf{C}\cdot d\tilde{\mathbf{W}}_t]_{\beta'}\\&=-\epsilon_{\mu\alpha\beta}\boldsymbol{\mathcal{R}}_{\beta\nu}\left[\mathbf{C}\cdot d\mathbf{W}_t\right]_\alpha\end{aligned} \tag{105}$$

which is the desired result (29).

[1] H. Goldstein, *Classical Mechanics* (Addison-Wesley, Massachusetts, 1983).
[2] K. V. V. I. Arnold, A. Weinstein, *Mathematical Methods Of Classical Mechanics*, Graduate Texts in Mathematics (Springer, 1989), 2nd ed.
[3] P. L. Lamy and J. A. Burns, American Journal of Physics **40**, 441 (1972).
[4] B. D. Warner, A. W. Harris, and P. Pravec, Icarus **202**, 134 (2009).
[5] S. Breiter, A. Rozek, and D. Vokrouhlický, Monthly Notices of the Royal Astronomical Society **427**, 755 (2012).
[6] S. X. Descamps, Quaderns d'Historia de l Enginyeria **9**, 270 (2008).
[7] W. Gautschi, SIAM review **50**, 3 (2008).
[8] P. Español, M. Thachuk, and J. De La Torre, European Journal of Mechanics - A/Solids **103**, 105184 (2024).
[9] S. Delong, Y. Sun, B.E. Griffith, E. Vanden-Eijnden, and A. Donev, Physical Review E **90**, 063312 (2014).
[10] A. Einstein, Ann. Phys. (Leipzig) **19**, 549 (1905).
[11] M. Green, J. Chem. Phys. **20**, 1281 (1952).
[12] R. Zwanzig, Physical Review **124**, 983 (1961).
[13] H. Grabert, *Projection Operator Techniques in Nonequilibrium Statistical Mechanics* (Springer, 1982).
[14] H. C. Öttinger, *Beyond Equilibrium Thermodynamics* (J. Wiley & Sons, 2005).
[15] J. W. Gibbs, *Elementary Principles in Statistical Mechanics* (Yale Univ. Press, 1902. Dover„ New York„ 1960).
[16] J. De La Torre and P. Español, European Journal of Mechanics - A/Solids p. 105298 (2024).
[17] L. Poinsot and C. Whitley, *Outlines of a New Theory of Rotatory Motion* (Creative Media Partners, LLC, 2022).
[18] L. D. Landau and E. M. Lifshitz, *Mechanics (Third Edition)* (Pergamon Press, 1960).
[19] M. S. Ashbaugh, C. C. Chicone, and R. H. Cushman, Journal of Dynamics and Differential Equations **3**, 67 (1991).
[20] O. Saporta Katz and E. Efrati, Physical Review Letters **122**, 024102 (2019).
[21] G. C. Price and D. Williams, in *Séminaire de Probabilités XVII 1981/82*, edited by J. Azéma and M. Yor (Springer Berlin Heidelberg, Berlin, Heidelberg, 1983), vol. 986, pp. 194–197.
[22] M. Van Den Berg and J. T. Lewis, Bulletin of the London Mathematical Society **17**, 144 (1985).
[23] F. Perrin, Journal de Physique et le Radium **5**, 497 (1934).
[24] W. H. Furry, Physical Review **107**, 7 (1957).
[25] L. D. Favro, Physical Review **119**, 53 (1960).
[26] P. S. Hubbard, Physical Review A **6**, 2421 (1972).
[27] F. Höfling and A. V. Straube, *Langevin equations and a geometric integration scheme for the overdamped limit of homogeneous rotational Brownian motion* (2024), arXiv 2403.04501.
[28] E. O. Díaz, *3D Motion of Rigid Bodies A Foundation for Robot Dynamics Analysis* (Springer, 2019).
[29] A. P. Thompson, H. M. Aktulga, R. Berger, D. S. Bolintineanu, W. M. Brown, P. S. Crozier, P. J. in 't Veld,

A. Kohlmeyer, S. G. Moore, T. D. Nguyen, et al., Comp. Phys. Comm. **271**, 108171 (2022).
[30] F. Pedregosa, G. Varoquaux, A. Gramfort, V. Michel, B. Thirion, O. Grisel, M. Blondel, P. Prettenhofer, R. Weiss, V. Dubourg, et al., Journal of Machine Learning Research **12**, 2825 (2011).
[31] E. Fermi, J. Pasta, and S. Ulam, *Studies of nonlinear problems. I. Los Alamos report LA-1940 (1955)*, published later in *Collected Papers of Enrico Fermi*, E. Segré (Ed.) (University of Chicago Press, Chicago 1965); also in Non- linear Wave Motion, Newell A. C. Ed., Lecture in Applied Mathematics 15 (AMS, Providence, Rhode Island, 1974); also in *The Many-Body Problem*, Mattis C. C. Ed. (World Scientific, Singapore, 1993).
[32] G. P. Berman and F. M. Izrailev, Chaos: An Interdisciplinary Journal of Nonlinear Science **15**, 15104 (2005).
[33] T. Dauxois, M. Peyrard, and S. Ruffo, European journal of physics **26**, S3 (2005).
[34] T. Dauxois, Physics Today **61**, 55 (2008).
[35] L. Martinetz, K. Hornberger, and B. A. Stickler, Physical Review E **97**, 052112 (2018).
[36] C. W. Gardiner, *Handbook of Stochastic Methods* (Springer-Verlag, Berlin, 1983).
[37] H. Risken, *The Fokker-Planck Equation* (Springer Verlag, Berlin, 1984).